



# Synthesis and evaluation of redox-sensitive gonadotropin-releasing hormone receptor-targeting peptide conjugates

Yuxuan Dai<sup>a</sup>, Na Yue<sup>a</sup>, Chunxia Liu<sup>a</sup>, Xingguang Cai<sup>a</sup>, Xin Su<sup>a</sup>, Xinzhou Bi<sup>a</sup>, Qifei Li<sup>a</sup>, Chengye Li<sup>a</sup>, Wenlong Huang<sup>a,b</sup>, Hai Qian<sup>a,b,\*</sup>

<sup>a</sup> Center of Drug Discovery, State Key Laboratory of Natural Medicines, China Pharmaceutical University, 24 Tongjiaxiang, Nanjing 210009, PR China

<sup>b</sup> Jiangsu Key Laboratory of Drug Discovery for Metabolic Disease, China Pharmaceutical University, 24 Tongjiaxiang, Nanjing 210009, PR China

## ARTICLE INFO

### Keywords:

Lytic peptides  
Redox-sensitive  
Membranolytic  
Apoptosis

## ABSTRACT

Lytic peptides have been demonstrated to exhibit obvious advantages in cancer therapy with binding ability toward tumor cells via electrostatic attractions, which are lack of active targeting and aggregation to tumor tissue. In the present study, five conjugated lytic peptides were redesigned and constructed to target gonadotropin releasing hormone receptors (GnRHR), meanwhile, the disulfide bridge was introduced to achieve redox sensitive delivery based on the experience from the preliminary work of lytic peptides P3 and P7. YX-1, was considered to be the most promising for in-depth study. YX-1 possessed high potency ( $IC_{50} = 3.16 \pm 0.3 \mu M$ ), low hemolytic effect, and cell membrane permeability in human A2780 ovarian cancer cells. Moreover, YX-1 had prominent pro-apoptotic activity by activating the mitochondria-cytochrome *c*-caspase apoptotic pathway. The study yielded the conjugate YX-1 with superior properties for antineoplastic activity, which makes it a promising potential candidate for targeting cancer therapy.

## 1. Introduction

Cancer is one of the most prevalent diseases diagnosed and one of the leading causes of mortality [1,2]. Although the advances in science and technology have led to developments in cancer therapeutic areas, the global cancer burden is expected to nearly double by 2030 [3,4]. Chemotherapy is one of the important approaches used in cancer therapy, but the toxicity of chemotherapeutics to normal cells remains an important obstacle in clinical application [5]. In addition, traditional cytotoxic chemotherapeutics could stimulate the multidrug resistance (MDR) phenotype [6], which involves the activation of a wide range of efflux pumps that expel the cytotoxic agents that harm them [5].

As a novel type of promising therapeutic, lytic peptides present significant advantages over traditional anti-cancer agents [7], such as little drug resistance [8] and slight toxicity to normal cells [9,10]. Lytic peptides are cationic and amphipathic in the innate immune system of nearly all multi-cellular and some single-cellular organisms [11,12]. Structurally, lytic peptides possess basic amino acids, such as arginine and lysine, and about half are hydrophobic amino acids, which could arrange into amphipathic structure and display potent cell-killing effect [8,13]. The cell membranes of cancer cells contain a high proportion of

net negative charges so that the cationic lytic peptides could selectively bind with cancer cells [14,15]. Therefore, the electrostatic and hydrophobic interactions between the peptides and cell membrane surface form the basis of these peptides' cytotoxicity [13]. Some structural optimized lytic peptides P3 (sequence: Leu-Val-Lys-Arg-Phe-Lys-Lys-Phe-Phe-Arg-Lys-Leu-Lys-Lys-Ser-Val-Leu-Leu-NH<sub>2</sub>) and P7 (sequence: Leu-Val-Arg-Arg-Phe-Arg-Arg-Phe-Phe-Arg-Arg-Leu-Arg-Arg-Ser-Val-Leu-Leu-NH<sub>2</sub>) have been designed which were endowed with better active and less toxic than their naturally occurring counterparts [16]. However, lytic peptides P3 and P7 are lack of active targeting to tumor tissue and could not aggregate to increase their concentration in tumor tissue.

Receptors that are expressed mainly on cancer cells symbolize attractive molecular targets for selective drug delivery [17]. The hormonal decapeptide gonadotropin-releasing hormone-I (GnRH-I; Glp-His-Trp-Ser-Tyr-Gly-Leu-Arg-Pro-Gly-NH<sub>2</sub>), released from the hypothalamus, plays a major role in the secretion of pituitary gonadotropin hormones [18,19]. Moreover, GnRH-I targets specific GnRH membrane receptors, which are characteristically overexpressed in many tumors including ovarian, breast, prostate and others, while its expression is scant in normal tissues [17,20]. GnRH-I and its enzyme

\* Corresponding author at: Centre of Drug Discovery, State Key Laboratory of Natural Medicines, China Pharmaceutical University, 24 Tongjiaxiang, Nanjing 210009, China.

E-mail address: [qianhai24@163.com](mailto:qianhai24@163.com) (H. Qian).

<https://doi.org/10.1016/j.bioorg.2019.102945>

Received 17 November 2018; Received in revised form 11 March 2019; Accepted 20 April 2019

Available online 29 April 2019

0045-2068/ © 2019 Elsevier Inc. All rights reserved.

stabilized analogs such as Triptorelin (D-Trp6-GnRH) have been used as a delivery vehicle to target cancer cells with overexpression of gonadotropin releasing hormone receptors (GnRHr) [21–24]. Targeted cancer therapies cause low systemic toxicities by precisely interfering molecules involved in the processes of tumor growth, progression, and spread [25]. The redox-heterogeneous microenvironment between normal cells and cancer cells has been well-studied to realize on-demand drug release [26]. Among them, disulfide bond bridge has been widely employed as typical reduction-responsive connection in the design of cancer-specific [27].

Here, we reported on the design, synthesis, and evaluation of novel conjugates containing the optimized lytic peptides P3, P7 and the well-known peptide KLL [8] directly attached or through a disulfide bond to Triptorelin. In vitro cytotoxicity evaluation indicated that five conjugates have improved anti-cancer effects on GnRHr-positive cancer cells. The conjugates YX-1, YX-3, YX-5 with reduction-sensitive disulfide bonds, exhibited favorable antitumor activity and membrane lysis activity, while YX-1 and YX-3 presented stronger functions and lesser side effects. Further investigations revealed that the conjugates YX-1 possessed the optimal biological properties which more gathered around ovarian cancer tissue. Subsequently, the disulfide bond was cleaved and the lytic peptides penetrated into cytoplasm and destroyed mitochondrial membranes, resulting in tumor cell apoptosis. Thus, YX-1 may be a promising potential for oncotherapy.

## 2. Results

### 2.1. Synthesis of GnRHr-targeting peptide conjugates

The five GnRHr-targeting peptide conjugates (Fig. 1) were successfully synthesized and purified by preparative RP-HPLC. The synthetic routes of the GnRHr-targeting peptides were illustrated in supporting information (Figs. S1, S2 and S4). All the derivatives displayed greater than 95% purity, and the identities of conjugates (Table S1 and Fig. S5) were confirmed by Waters ACQUITY UPLC–MS Systems.

### 2.2. Toxicity of the GnRHr-targeting peptide conjugates on cancer cells

Although the cytotoxic activity of lytic peptides on cancer cells has been previously described, these peptides possess weak cancer targeting [16]. The cytotoxicity activities of the conjugates were evaluated on various cell lines (Table 1). The expression of GnRHr in respective cell lines was confirmed by Western blot analysis. All the conjugates exhibited improved cytotoxic effects on the ovary cancer cells and breast cancer cells which overexpress GnRHr, especially for A2780. The conjugates showed great selectivity of cytotoxicity against cancer cells, with a 4- to 12-fold difference of  $IC_{50}$  values between cancer and normal cells (Table 1). According to the results, the potency of

conjugates against cancer cell lines were better than that of former lytic peptides (P3 and P7), suggesting that the conjugation strategy was proven to be practical. Furthermore, it could be speculated that the increased cytotoxicity of the conjugates may be mediated by the GnRHr. Moreover, YX-1 and YX-3 of which the structure contained disulfide-bond-bridged exerted stronger anti-cancer activity over YX-2 and YX-4. All the conjugates showed weak toxicity to the normal cell lines. The data also exhibited almost equal potency to both drug-resistant and -sensitive cells.

### 2.3. Expression level of GnRHr in each cell

The expression of GnRHr was accomplished by western blots analysis. As presented in Fig. 2, the results showed that A2780 and SKOV3 had higher expression quantities of GnRHr protein than that of other cells and A2780 was the highest. Meanwhile, as shown in Table 1, YX-1 and YX-3 showed significant potency against A2780 and SKOV3 and possessed stronger cytotoxic activity in A2780 than SKOV3. The data was consistent with the result of Fig. 2. Subsequently, A2780 cell line was utilized for the remainder of the mechanism studies.

### 2.4. The competitive binding assay of the GnRH-targeting peptide conjugates

To determine if the GnRHr mediation of the conjugates was an underlying cause for the increased cytotoxicity, we created GnRHr competitive binding assay. Triptorelin, a kind of a typical GnRHr agonist which possesses high GnRHr binding affinity. Meanwhile, Gtetrorelix is a kind of GnRHr antagonist. Thus, we employed Triptorelin and Cetrorelix as the competitive molecules. The A2780 and K562 cells were exposed to the conjugates in increasing concentrations (0–40  $\mu$ M). The conjugates exhibited a dose-dependent decrease in cell proliferation. In the control cell line K562, which has lower expression of GnRHr, no significant reduction of cytotoxic activity of GnRHr-targeting conjugates was observed while pretreated with Triptorelin (10  $\mu$ M) or Cetrorelix (10  $\mu$ M). Moreover, The  $IC_{50}$  values for A2780 cells were  $3.27 \pm 0.78 \mu$ M for YX-1 and  $3.98 \pm 0.27 \mu$ M for YX-3, respectively (Fig. 3). Addition of Triptorelin (10  $\mu$ M) increased the  $IC_{50}$  concentrations to  $7.34 \pm 0.89 \mu$ M for YX-1 and  $9.13 \pm 0.49 \mu$ M for YX-3. Addition of Cetrorelix (10  $\mu$ M) increased the  $IC_{50}$  concentrations to  $8.00 \pm 0.63 \mu$ M for YX-1 and  $10.56 \pm 0.97 \mu$ M for YX-3. The results suggested that Triptorelin or Cetrorelix has competitive effect with GnRH-targeting conjugates. In other words, the cell growth inhibitory effects of the conjugates were GnRHr dependent.

### 2.5. GnRH-targeting peptide conjugates disrupted cytoplasmic membrane

To investigate if the conjugates retained property with the disruptive membrane of lytic peptides, we designed lactate dehydrogenase

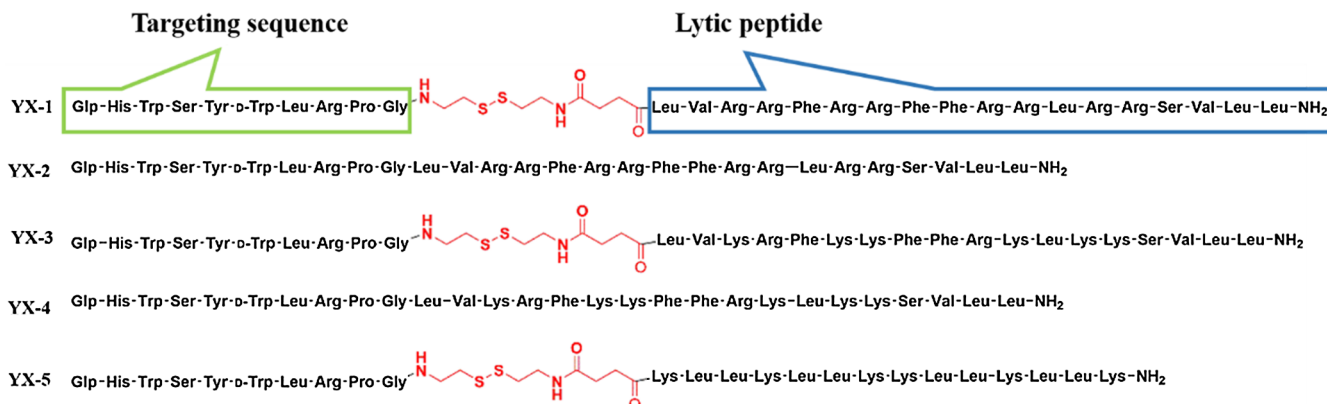
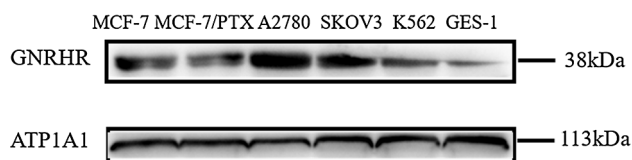


Fig. 1. Chemical structures of GnRHr-targeting peptide conjugates. Glp means pyroglutamic acid.

**Table 1**  
Anti-tumor activity of the conjugates.<sup>a</sup>

Compounds	IC <sub>50</sub> (μM)					
	MCF-7	MCF-7/PTX	K562	A2780	SKOV3	GES-1
YX-1	7.34 ± 0.31	9.05 ± 0.62 <sup>*</sup>	7.59 ± 0.46	3.16 ± 0.30 <sup>*</sup>	5.16 ± 0.62 <sup>*</sup>	55.56 ± 2.18
YX-2	9.55 ± 0.96	22.05 ± 1.58	9.82 ± 0.37	4.18 ± 0.15 <sup>*</sup>	6.14 ± 0.79 <sup>*</sup>	48.26 ± 1.23
YX-3	7.83 ± 0.72	9.56 ± 0.61 <sup>#</sup>	8.23 ± 0.65 <sup>#</sup>	3.94 ± 0.07 <sup>#</sup>	4.91 ± 0.41 <sup>#</sup>	53.31 ± 1.79
YX-4	10.9 ± 0.48	24.05 ± 1.13	8.37 ± 0.31 <sup>#</sup>	4.48 ± 0.08 <sup>#</sup>	5.79 ± 0.38 <sup>#</sup>	47.28 ± 2.05
YX-5	9.97 ± 0.85	8.49 ± 0.74	7.54 ± 0.74	5.14 ± 0.27 <sup>*,#</sup>	5.19 ± 0.82 <sup>*,#</sup>	37.47 ± 1.58
P3	11.23 ± 1.01	13.31 ± 1.05	16.17 ± 1.28 <sup>#</sup>	14.75 ± 0.83	14.08 ± 1.04	44.15 ± 2.63
P7	9.17 ± 0.47	15.2 ± 1.12	9.46 ± 0.26	10.68 ± 0.25	13.91 ± 1.17	55.24 ± 2.41
PTX	0.81 ± 0.09	59.4 ± 3.21	0.73 ± 0.04	3.62 ± 0.04	5.41 ± 0.19	9.27 ± 1.12

<sup>a</sup> Notes: <sup>\*</sup>P < 0.05, (compared to P7); <sup>#</sup>P < 0.05, (compared to P3); PTX: paclitaxel. A2780 and SKOV3: human ovarian cancer cell lines; MCF-7 and MCF-7/PTX: human breast cancer cell lines; K562: leukemia cell line; GES-1: human gastric mucosal epithelial cell line.



**Fig. 2.** Expression level of GnRHr in various cancer.

(LDH) leakage assay as previously reported [16]. Membrane lysis activity of the conjugates confirmed by measuring release of the ubiquitous, cytoplasmic enzyme LDH in the culture medium. A2780 cells were incubated with different concentrations of peptides (YX-1, YX-2, YX-3, YX-4 and YX-5) and the results exhibited that the conjugates caused the release of the cytosolic enzyme LDH in a concentration-dependent manner (Fig. 4A). Notably, as illustrated in Table 1 and Fig. 2, YX-1, YX-3 and YX-5 possessed greater anti-cancer activity in A2780 cells and stronger disruptive membrane activity. To further validate these effects observed, fluorescent dyes AO and EB were utilized to detect membrane integrity in A2780 cells. As shown in Fig. 4B, A2780 cells displayed red fluorescence all after treatment with the conjugates (2 μM of YX-1, and 3 μM of YX-3,) for 1 h.

Thus, these results demonstrated that the conjugates (YX-1, YX-3 and YX-5) with the character of lytic peptides could disrupt the membrane and alter the penetrability to strengthen the cytotoxicity activity of conjugates.

## 2.6. Hemolytic activity

Many lytic peptides could induce hemolysis, which prevents their clinical application [8,28]. To assess the safety profile of the designed conjugates, we examined their hemolytic activity using RBCs. As depicted in Fig. 5, the conjugates YX-5 showed strong hemolytic properties, while its counterpart, YX-1 and YX-3 with linking the lytic peptides P3 and P7 to Triptorelin by disulfide bridge bond had little hemolytic activity compared to the conjugate YX-5.

## 2.7. Redox response sensitivity

Compared to normal cells, tumor cells simultaneously overproduce glutathione (GSH), leading to a redox intracellular environment [29,30].

Disulfide bonds have been widely applied to typical reduction-sensitive linkages in the design of cancer-specific stimuli-responsive [27]. Our group developed disulfide-bridged reduction-sensitive targeting GnRHr conjugates for cancer therapy. The conjugate with structure of CS had a disulfide bond that could be cleaved by reductants such as GSH. As indicated by the LC-MS results that almost 80% mol of the original conjugates (YX-1, YX-3) been converted when GSH (5 mM) triggered the disulfide bond cleavage in or within approximately 10 min (Fig. 6).

## 2.8. The cell penetration and pro-apoptotic ability of GnRHr targeting conjugates in cancer cells

To characterize the ability of conjugates to penetrate cells, FITC labeled conjugates were synthesized (Table S2). YX-3<sub>FITC</sub> and YX-4<sub>FITC</sub> showed improvement of their cell penetration ability as compared to P3<sub>FITC</sub> in A2780 cells. This is probably due to introduction of the targeting sequence which might facilitate cell penetration. Notably, YX-3<sub>FITC</sub> showed the highest efficiency in cell penetration (Fig. 7A and B). The apoptotic effects of the conjugates were assessed by Annexin-FITC/PI staining and the percentage of apoptotic A2780 cells was detected by flow cytometry analysis. As shown in Fig. 7C, in the control group, the activation of apoptosis of A2780 cells were insignificant. Nevertheless, 1, 2 and 4 μM of YX-1 induced 8.3, 17.9 and 47.3% A2780 cell apoptosis, while YX-3 with the same concentration induced 5.4, 12.5 and 32.5% A2780 cell apoptosis, respectively. These results showed that the activation of apoptotic effect of YX-1 and YX-3 presented to be a concentration dependent manner and YX-1 possessed stronger pro-apoptotic activity compared to YX-3.

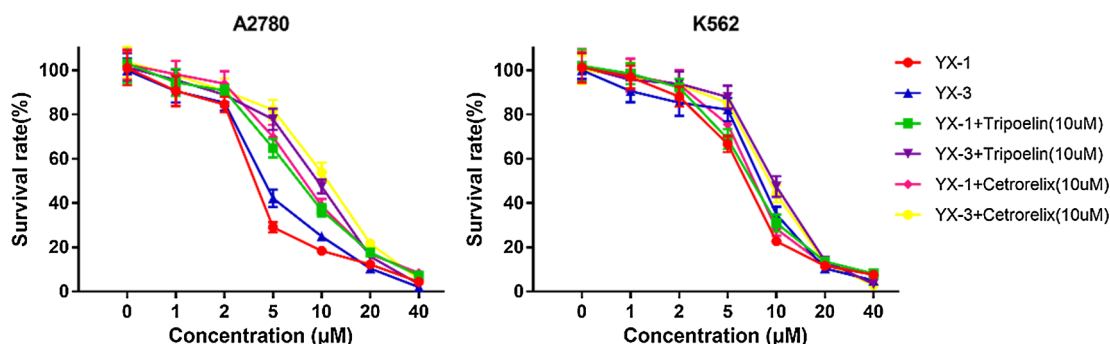


**Fig. 3.** GnRHr competitive binding assay.

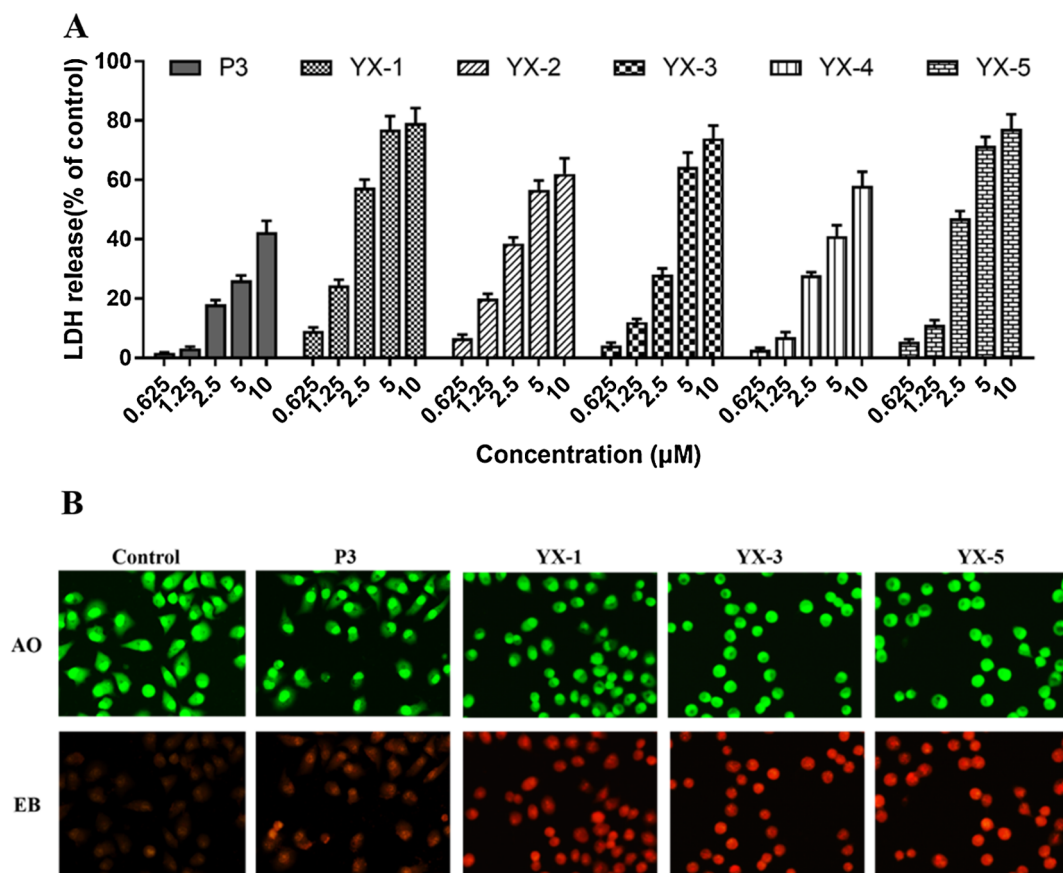


Fig. 4. (A) LDH leakage assay of GnRH-targeting peptide conjugates; (B) AO/EB staining images of A2780 cells after treatment with P3 (6 μM), YX-1 (2 μM) and YX-3 (3 μM), respectively.

### 2.9. Mitochondrial membrane potential assay and mechanism of conjugates

The change of mitochondrial membrane potential, the essential parameter of cell apoptosis [31], was determined with the mitochondrial membrane potential-sensitive dual-emission probe JC-1 (Sigma-Aldrich). JC-1 accumulates in healthy mitochondria, where it forms J-aggregates that display orange fluorescence. While the mitochondrial membrane is depolarized, JC-1 exists as a monomer and displays green fluorescence. As shown in Fig. 8, red fluorescence diminished and green fluorescence was augmented after treatment with 6 μM of P3, 2 μM of YX-1 and 3 μM of YX-3. The observations demonstrated that the conjugates performed a role in the dissipation of mitochondrial membrane potential and caused the mitochondrial depolarization.

### 2.10. Expression level of and Cytochrome-C Caspase-3

We tested whether treatment with YX-1 and YX-3 activated Caspase-3- Cytochrome-C apoptotic pathway which is a key step in the performance of cell apoptosis [32–34]. In this study, the alteration of caspase-3 and Cytochrome-C were determined by western blot in A2780 cells. As shown in Fig. 9A and B, treatment with 2 μM of YX-1, 3 μM of YX-3 and 6 μM of P3 for 1 h, led to a significant increase of cleaved caspases-3 and Cytochrome-C levels in the cytoplasm.

## 3. Discussion

Recently, the application of hormonal peptide like GnRH or its analogs for drug targeting of cancer therapy has intensively been investigated. In this study, we chosen the lytic peptides P3 and P7 as the

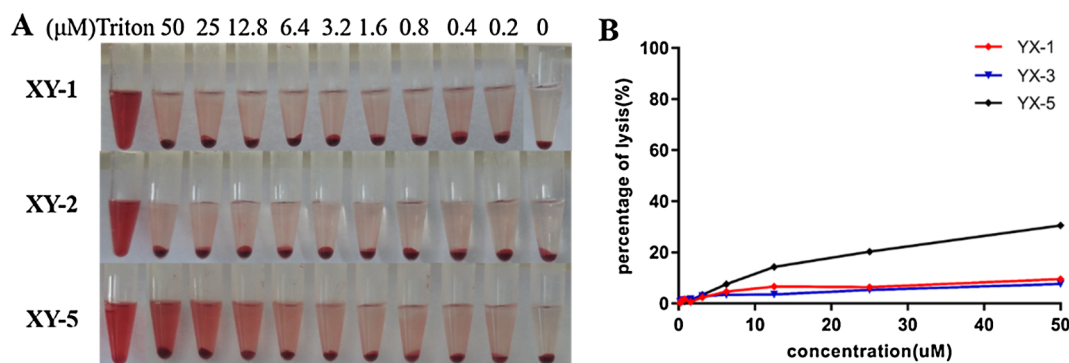


Fig. 5. (A) Hemolysis effects on RBCs of XY-1, XY-3 and XY-5; (B) Quantitative data from the hemolysis measurement described in (A).

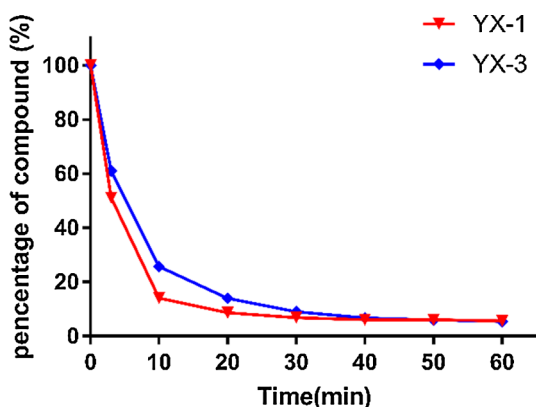


Fig. 6. The redox response sensitivity of YX-1 and YX-3.

cytotoxic part and Triptorelin as the targeting part, meanwhile, the disulfide bond was introduced as reductive-sensitive linker. Thus, five novel GnRH-conjugated peptides were designed, which were utilized to target and destroy ovarian cancer (Fig. 1).

The result of cell viability assay showed that all the conjugates had improved cytotoxic activity in cancer cells expressing high levels of GnRHr, and the conjugates YX-1 ( $IC_{50} = 3.16 \pm 0.30 \mu M$ ) and YX-3 ( $IC_{50} = 3.94 \pm 0.07 \mu M$ ) exhibited stronger property against A2780 ovarian cancer cells (Table 1). The following receptor competitive binding assay showed that pre-incubation Triptorelin could reduce the anti-proliferation activity of conjugates against A2780 cells (Fig. 3). This finding indicated that the increased cytotoxicity relied on GnRHr.

Next, the research was conducted to verify the membrane-disrupting effects of conjugates, and LDH leakage assay suggested that YX-1 and YX-3 presented stronger membrane disrupting activity against A2780 cells in a concentration-dependent manner. The visualization of AO/EB double staining test also corroborated evidence of the disruption to A2780 cell membranes (Fig. 4). YX-1 and YX-3 conjugates were selected for further investigation. Meanwhile, YX-1 and YX-3 exhibited little hemolysis activity against the RBCs (Fig. 5).

The chemical bond between Triptorelin and lytic peptides should exhibit specific rupture in the tumor microenvironment (GSH concentration: 5–10 mM). Thus, redox response sensitivity assay proved that the conjugates YX-1 and YX-3 could be broken rapidly to achieve targeting delivery (Fig. 6). The in depth mechanism associated with the anti-tumor activity of conjugates remained to be investigated.

After penetrating into the cytoplasm, lytic peptides make contact with mitochondria and destroy mitochondrial membranes, resulting in mitochondrial membrane depolarization, leakage of Cytochrome-C into the cytosolic compartment and apoptosis. Therefore, cell penetration ability was evaluated by FITC-labeled conjugates, mitochondria membrane disrupting effect was determined by using JC-1 assay, and the pro-apoptotic effect was further confirmed by Annexin V-FITC/PI apoptosis test. Meanwhile, we quantified leakage of Cytochrome-C and active caspase-3 by western-blot method. According to the JC-1 assay, images showed that red fluorescence changed to green after treatment with YX-1 and YX-3. The loss of mitochondrial membrane potential is a prelude to cell apoptosis (Fig. 8). Meanwhile, YX-1 and YX-3 were capable of increasing the cytochrome C contents in the cytoplasm versus control and activating caspase 3, an effector caspase that is responsible for apoptotic destruction of the cells (Fig. 9). The Annexin-FITC/PI staining proved that the pro-apoptosis proportion of YX-1 was greater than that of YX-3 with a dose-dependent manner (Fig. 7). Notably, the results suggested that YX-1 was the most suitable candidate for subsequent treatment.

In summary, we conclude that the anti-cancer mechanisms of GnRH-targeting peptide conjugates can be divided into four steps (Fig. 10): (1) targeting the cancer cells with high expression of GnRH and aggregation in a field nearby; (2) penetration of cancer cells with

more anionic membranes; (3) cleavage of disulfide bridge to release the lytic peptides; (4) penetration into the cytoplasm by virtue of the disrupted membrane; (5) disruption of mitochondrial membranes, release of cytochrome C and induction of caspase-3-dependent apoptotic cell death.

#### 4. Conclusion

We designed a panel of GnRHr targeting conjugates possessed reductive-sensitive and elucidated the action mechanism of anti-cancer activity. Further investigation revealed that YX-1, the conjugate containing Triptorelin sequence, exhibited the most potency in tumor cells, and showed great promise with significant advantages of human A2780 ovarian cancer cells. The present work signifies that the conjugate YX-1 possesses targetability, high specificity and cell membrane permeability and promotes apoptosis, may be a promising candidate for cancer therapy.

#### 5. Experimental section

##### 5.1. synthesis, purification and analysis of conjugates

All peptide fragments were synthesized using standard 9-fluorenylmethoxycarbonyl (Fmoc) solid phase synthesis techniques. Briefly, the lytic membrane peptide segments (P3, P7 and KLL) were prepared on Fmoc-Rink Amide MBHA resin. The general procedure of peptide preparation has been reported previously [16,35]. The targeting segments (sequence: Glp-His-Trp-Ser-Tyr-<sub>n</sub>-Trp-Leu-Arg-Pro-Gly) with protecting groups were achieved on 2-chlorotrityl chloride resin (Fig. S1). The linker with disulfide bond was obtained by two steps reaction. Cystamine was firstly reacted with succinic anhydride and then with Fmoc-OSu to produce Fmoc-Cystamine Succinate (Fmoc-CS).

Fmoc-CS, white solid; yield, 36%.  $^1H$  NMR (300 MHz, DMSO- $d_6$ )  $\delta$  8.14 (s, 1H, NH);  $\delta$  7.88–7.90 (d,  $J = 6.00$  Hz, 2H, ArH); 7.68–7.70 (d,  $J = 6.00$  Hz, 2H, ArH); 7.39–7.44 (t, 2H, ArH); 7.31–7.35 (m, 2H, ArH); 6.28 (s, 1H, NH); 4.30–4.32 (d,  $J = 6.30$  Hz, 2H, OCH<sub>2</sub>); 4.22–4.23 (m, 1H, CH); 3.06–3.34 (m, 4H, 2  $\times$  CH<sub>2</sub>); 2.50–2.76 (m, 4H, 2  $\times$  SCH<sub>2</sub>); 2.23–2.35 (m, 4H, 2  $\times$  CH<sub>2</sub>). MS (ESI)  $m/z$  calcd for [C<sub>32</sub>H<sub>26</sub>N<sub>2</sub>O<sub>5</sub>S<sub>2</sub> + Na]<sup>+</sup> 497.6, found 497.7.

Then conjugates were prepared by SPPS using Fmoc-CS and other Fmoc-amino acids with side chains properly protected. The synthetic route of conjugate YX-1 as depicted in Fig. S2. For peptides YX-3 and YX-4, the Dde protection of Lys was removed by hydrazine/DMF (2%, v/v) for 3 times for 10 min at 25 °C. The result was detected by Kaiser test. Then Fmoc- $\beta$ -Ala-OH was coupled. Fmoc group was removed and FITC labeling was performed with the solution of FITC (4 equiv) and DIPEA (12 equiv) in DMF in the dark overnight. All crude conjugates were purified by preparative RP-HPLC (Shimadzu LC-10) with C18 column (5  $\mu m$ , 340  $\times$  28 mm) and then characterized by UPLC/MS (Waters UPLC with the ACQUITY TQD; Waters Corporation, Milford, MA, USA) with a Waters ACQUITY UPLCBEH C18 column (1.7  $\times$  50 mm, Waters). The purity of the conjugates was above 95%.

##### 5.2. Cell cultures

Human ovarian A2780 and SKOV3 cancer cell lines, human breast MCF-7 cancer cell lines, paclitaxel resistant sub-line MCF-7/PTX, leukemia K562 cells, and human gastric mucosal epithelial cells GES-1 were obtained from KeyGEN BioTECH (Nanjing, China). K562 and GES-1 cells were cultured in RPMI 1640 supplemented with 10% fetal calf serum (FBS, Hyclone Laboratories) and 1% penicillin/streptomycin antibiotics (GibcoBRL). MCF-7, MCF-7/PTX and A2780 cells were cultured in DMEM supplemented with 10% FBS and 1% antibiotics. SKOV3 cells were cultured in McCoy's 5A supplemented with 10% FBS and 1% antibiotics. All the cells were incubated in a humidified incubator at 37 °C with 5% CO<sub>2</sub>.

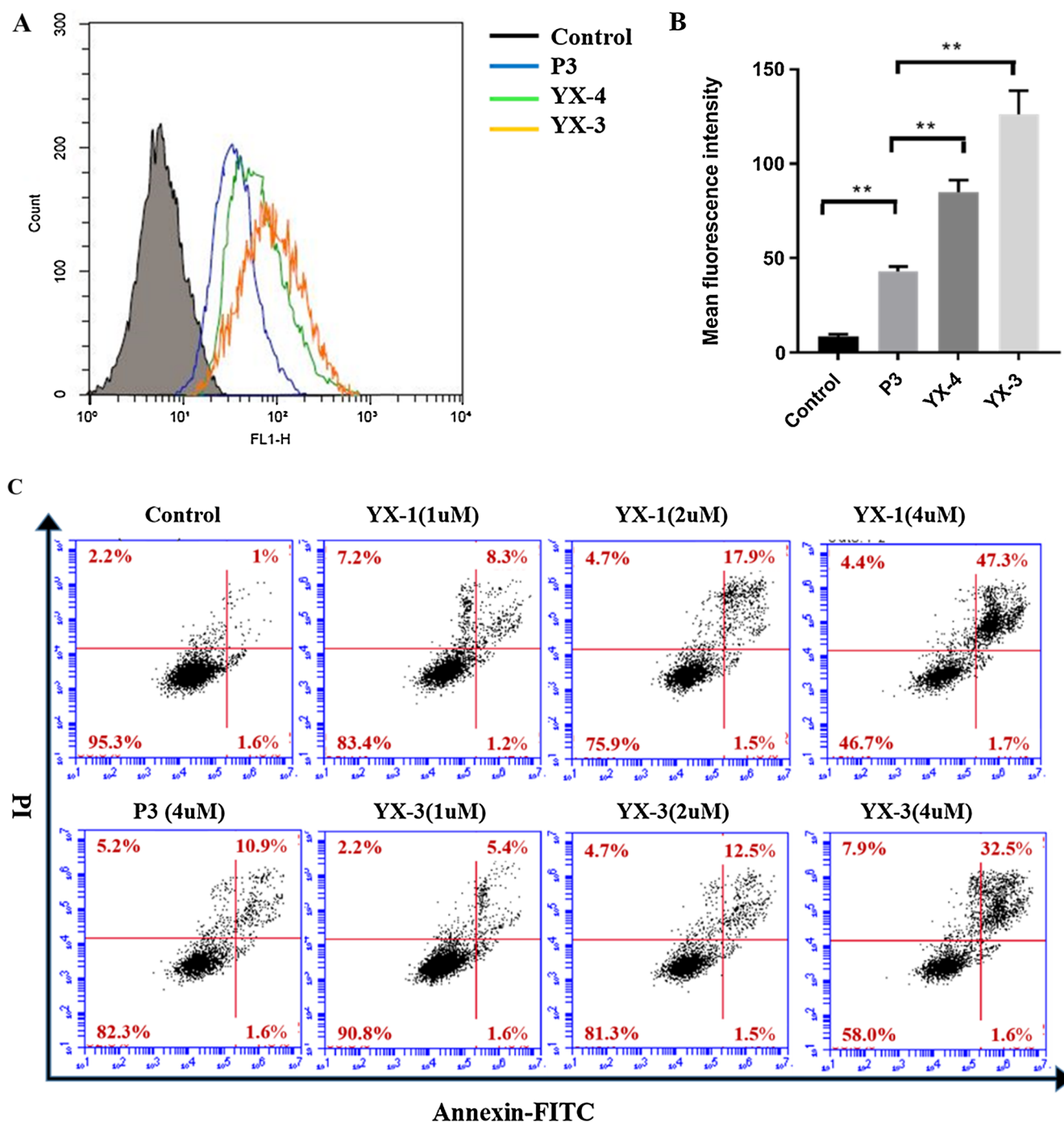


**Fig. 7.** (A) Uptake of P3, YX-3 and YX-4 in A2780 cells. Cells were incubated with serum-free medium or medium containing 2  $\mu$ M FITC labeled conjugates for 30 min; (B); Mean fluorescence intensity of the flow plots of (A); (C) The effects of compounds on A2780 cell apoptosis using Annexin-FITC/PI staining assay.

### 5.3. Cell proliferation and viability assay

We used a methylthiazol tetrazolium (MTT) assay to evaluate the cytotoxicity of the conjugates in various cell lines. Cells were seeded in 96-well plates at a density of  $6 \times 10^3$  cells/well and were grown for 12 h before treatment. The medium was then substituted with serum-free medium containing various concentrations of conjugates. After 48 h of incubation, 20  $\mu$ L of 5 mg/ml MTT solution was added to each well and the plates were cultured for another 4 h at 37  $^{\circ}$ C. Next, 150  $\mu$ L of DMSO was added to each well for dissolving the purple formazan precipitate. The absorbance of each sample at 490 nm was determined by a microplate reader (Bio-Rad, iMark 680). The  $IC_{50}$  values were

estimated from sigmoidal regressions with Graph Pad Prism 7.0 software.

### 5.4. Hemolysis assay

Wistar rats (male, 180–220 g, Certificate number: NO.201824693) were purchased from the Comparative Medical Center of Yangzhou University (Jiangsu, China). All the animals involved were treated in accordance with protocols approved by the ethical committee of China Pharmaceutical University. All animal experimental protocols adhered to the Guide for the Care and Use of Laboratory Animals published by the National Institutes of Health (NIH publication 85–23, revised 1986).

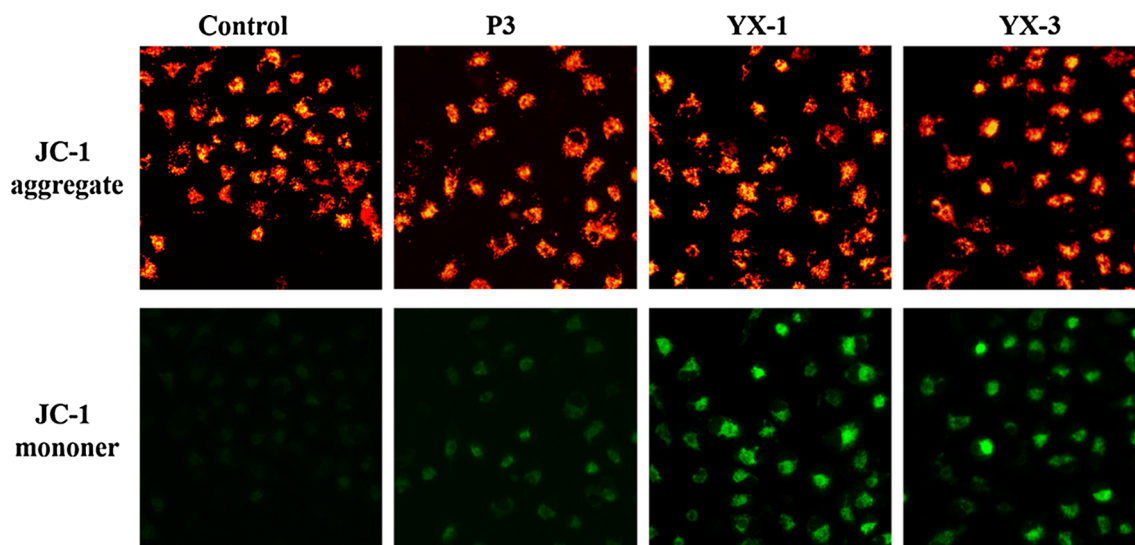


Fig. 8. Conjugates induced the alternation of mitochondrial membrane potential. JC-1 staining images of A2780 cells after treatment with P3 (6  $\mu\text{M}$ ), YX-1 (2  $\mu\text{M}$ ) and YX-3 (3  $\mu\text{M}$ ), respectively.

Red blood cells (RBCs) isolated from fresh mouse blood were collected and washed two times with 0.9% saline. The RBCs were diluted to  $5 \times 10^8/\text{mL}$ , and 250  $\mu\text{L}$  of these RBCs were incubated with various concentrations of conjugates at 37  $^\circ\text{C}$  for 1 h. The diluted RBC suspension was mixed with PBS buffer as a negative control, 1% Triton X-100 as a positive control. Then, the groups were centrifuged at 2000g for 10 min, and the supernatants from each group were measured by absorbance at 540 nm in a microplate reader (Bio-Rad, iMark 680). Assays were examined three times.

#### 5.5. Cytoplasmic enzyme lactate dehydrogenase (LDH) release assay

The LDH leakage assay was used to determine the membrane integrity by using a commercial LDH Activity Assay Kit (Nanjing Jiancheng Bioengineering Institute) [36]. The LDH assay was accomplished according to the manufacturer's protocols. Briefly, A2780 cells were seeded in a 96-well plate ( $6 \times 10^3$  cells per well) and cultured for 24 h. Next, the serum-free medium containing the various concentrations of conjugates was added and incubated for 12 h. The plates were centrifuged (3000g, 10 min) and Cell-free culture supernatants were transferred to a new 96-well plate. PBS buffer was added as a negative control which was taken as no leakage. The absorbance was detected by microplate reader at 450 nm. The cells treated with 1% Triton X-100 represented 100% leakage.

#### 5.6. Acridine orange/ethidium bromide (AO/EB) double staining

A2780 cells was used for AO/EB double staining. Briefly, A2780 cells were grown in a 12-well plate at  $2 \times 10^5$  cells per well, cultured for 24 h. Then the cells were treated with 2  $\mu\text{M}$  of YX-1 and 3  $\mu\text{M}$  of YX-3 for 1 h, respectively. Next, the cells were stained with 20  $\mu\text{g}/\text{ml}$  of

AO/EB solution in the dark for 10 min. Subsequently, excess AO/EB dye mixture was washed with cold PBS. Fluorescence images were obtained with fluorescence microscopy (Nikon Ts2R).

#### 5.7. Mitochondrial membrane potential ( $\Delta\psi_m$ ) assay

The mitochondrial membrane potential was estimated using the mitochondrial Membrane Potential Assay Kit (Beyotime Biotechnology). Concisely, A2780 cells were grown at 80% confluency in a 6-well plate and were incubated with YX-1 (2  $\mu\text{M}$ ), YX-3 (3  $\mu\text{M}$ ) and vehicle for 4 h and stained with JC-1 according to the protocol. The images were taken by fluorescence microscope (Nikon Ts2R).

#### 5.8. Cellular Uptake and Annexin V-FITC/propidium iodide (PI) apoptosis assay

Adherent A2780 cells were seeded overnight in 6-well plates and then treated with 2  $\mu\text{M}$  FITC labeled compounds in FBS-free medium for 2 h at 37  $^\circ\text{C}$ . Then cells were collected and washed with PBS for three times. The cellular fluorescence intensities of about 10,000 cells treated by respective compounds were analyzed each time using a flow cytometer. Apoptotic cells were quantitated by flow cytometry with annexin V-FITC/PI Detection Kit (Nanjing Jiancheng Bioengineering Institute). A2780 cells were seeded in a 6-well plate and cultured overnight. Next, the cells were incubated with different concentrations of conjugates (YX-1 and YX-3), or vehicle for 12 h and were later processed according to the manufacturer's instructions. Flow cytometry was used to analyze the percentage of apoptotic cells (Beckman Coulter Accuri C6).

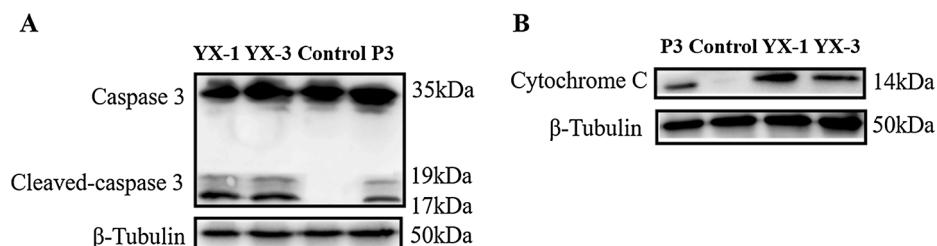


Fig. 9. (A) The western blot analysis of Caspase-3 for A2780 cells; (B) The western blot analysis of Cytochrome C.  $\beta$ -Tubulin was probed as loading control.

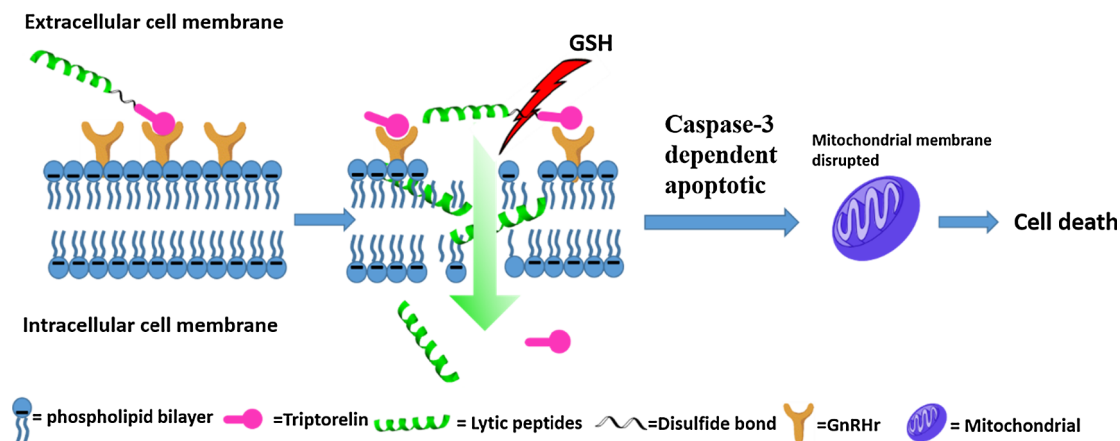


Fig. 10. The schematic diagram of the proposed anti-cancer mechanism of GnRHr targeting peptide conjugates.

### 5.9. Western blot

A2780 cells were plated in a 6-well plate at a density of  $6 \times 10^5$  cells/well and were cultured for 24 h. The cells were then treated with  $2 \mu\text{M}$  of YX-1 or YX-3 for 30 min. The mediums containing conjugates was removed, and the cells were washed with cold PBS. The membrane protein was obtained using Membrane Protein Extraction Kit (Nanjing Jiancheng Bioengineering Institute). All of the samples were resolved on 6–12% Bis-Tris acrylamide gels (Macklin), followed by transfer to a PVDF membrane. The membranes were blocked in 5% nonfat dry milk for 1.5 h at room temperature and incubated with rabbit polyclonal antibody (CASP3 polyclonal antibody, ABclonal; CYCS Polyclonal Antibody, ABclonal;  $\beta$ -Tubulin polyclonal antibody, ABclonal) at  $4^\circ\text{C}$  overnight. Next, the PVDF membranes were washed three times with TBST, followed by incubation with goat anti-rabbit IgG (H + L) HRP (Multi sciences) for 2 h at room temperature. The blots were washed using TBST three times at 5 min intervals. The protein bands were displayed using Tanon High sig ECL western blotting and a luminescent image analyzer (Tanon 5500).

### 5.10. Statistical analysis

Data were calculated using Microsoft Excel 2007 and/or GraphPad Prism 7.0. Data were presented as mean  $\pm$  SD for three independent tests. Comparisons among groups were statistically analyzed by one-way analysis of variance (ANOVA). P values  $< 0.05$  were considered significant.

### Acknowledgements

This work was supported by the National Natural Science Foundation of China (No. 81872734 & No. 81673299).

### Conflict of interest

The authors have no conflicts of interest to declare.

### Appendix A. Supplementary material

Supplementary data to this article can be found online at <https://doi.org/10.1016/j.bioorg.2019.102945>.

### References

- [1] R.L. Siegel, K.D. Miller, A. Jemal, *Cancer statistics, 2017*, *Ca-a Cancer J. Clinicians* 67 (2017) 7–30.
- [2] B.A. Miller, *Cancer statistics review 1973-1989*.
- [3] J. Heymach, L. Krilov, A. Alberg, N. Baxter, S.M. Chang, R. Corcoran, W. Dale, A. DeMichele, C.S.M. Diefenbach, R. Dreicer, A.S. Epstein, M.L. Gillison, D.L. Graham, J. Jones, A.H. Ko, A.M. Lopez, R.G. Maki, C. Rodriguez-Galindo, R.L. Schilsky, M. Sznol, S.N. Westin, H. Burstein, *Clinical cancer advances 2018: annual report on progress against cancer from the American Society of Clinical Oncology*, *J. Clin. Oncol.* 36 (2018) 1020–+.
- [4] L. Marcu, E. Bezak, B.J. Allen, *Global comparison of targeted alpha vs targeted beta therapy for cancer: In vitro, in vivo and clinical trials*, *Crit. Rev. Oncol. Hematol.* 123 (2018) 7–20.
- [5] Q. Wu, Z. Yang, Y. Nie, Y. Shi, D. Fan, *Multi-drug resistance in cancer chemotherapy: Mechanisms and lab approaches*, *Cancer Lett.* 347 (2014) 159–166.
- [6] D. Waghray, Q. Zhang, *Inhibit or evade multidrug resistance P-glycoprotein in cancer treatment*, *J. Med. Chem.* 61 (2018) 5108–5121.
- [7] H.-L. Chu, B.-S. Yip, K.-H. Chen, H.-Y. Yu, Y.-H. Chih, H.-T. Cheng, Y.-T. Chou, J.-W. Cheng, *Novel antimicrobial peptides with high anticancer activity and selectivity*, *PLoS ONE* 10 (2015).
- [8] X. Liu, R. Cao, S. Wang, J. Jia, H. Fei, *Amphipathicity determines different cytotoxic mechanisms of lysine- or arginine-rich cationic hydrophobic peptides in cancer cells*, *J. Med. Chem.* 59 (2016) 5238–5247.
- [9] A.L. Hilchie, A.J. Sharon, E.F. Haney, D.W. Hoskin, M.B. Bally, O.L. Franco, J.A. Corcoran, R.E.W. Hancock, *Mastoparan is a membranolytic anti-cancer peptide that works synergistically with gemcitabine in a mouse model of mammary carcinoma*, *Biochim. Biophys. Acta-Biomembranes* 1858 (2016) 3195–3204.
- [10] J.R. Vargas, E.G. Stanzl, N.N.H. Teng, P.A. Wender, *Cell-penetrating, guanidinium-rich molecular transporters for overcoming efflux-mediated multidrug resistance*, *Mol. Pharm.* 11 (2014) 2553–2565.
- [11] K.-Y. Choi, L.N.Y. Chow, N. Mookherjee, *Cationic host defence peptides: multifaceted role in immune modulation and inflammation*, *J. Innate Immun.* 4 (2012) 361–370.
- [12] W. Huang, J. Seo, S.B. Willingham, A.M. Czyzewski, M.L. Gonzalgo, I.L. Weissman, A.E. Barron, *Learning from host-defense peptides: cationic, amphipathic peptoids with potent anticancer activity*, *PLoS ONE* 9 (2014).
- [13] N.W. Schmidt, A. Mishra, G.H. Lai, M. Davis, L.K. Sanders, D. Tran, A. Garcia, K.P. Tai, M.C. Jr, A.J. Ouellette, *Criterion for amino acid composition of defensins and antimicrobial peptides based on geometry of membrane destabilization*, *J. Am. Chem. Soc.* 133 (2011) 6720–6727.
- [14] W.C. Wimley, *Describing the mechanism of antimicrobial peptide action with the interfacial activity model*, *ACS Chem. Biol.* 5 (2010) 905–917.
- [15] C.B. Falcao, C. Perezpeinado, B.G.D. La Torre, X. Mayol, H. Zamoracarreras, M.A. Jimenez, G. Radisbaptista, D. Andreu, *Structural dissection of crotalicidin, a rattlesnake venom cathelicidin, retrieves a fragment with antimicrobial and anti-tumor activity*, *J. Med. Chem.* 58 (2015) 8553–8563.
- [16] Y. Dai, X. Cai, W. Shi, X. Bi, X. Su, M. Pan, H. Li, H. Lin, W. Huang, H. Qian, *Proapoptotic cationic host defense peptides rich in lysine or arginine to reverse drug resistance by disrupting tumor cell membrane*, *Amino Acids* 49 (2017) 1601–1610.
- [17] P. Xu, Y. Jia, Y. Yang, J. Chen, P. Hu, Z. Chen, M. Huang, *Photodynamic oncotherapy mediated by gonadotropin-releasing hormone receptors*, *J. Med. Chem.* 60 (2017).
- [18] R.P. Millar, Z.L. Lu, A.J. Pawson, C.A. Flanagan, K. Morgan, S.R. Maudsley, *Gonadotropin-releasing hormone receptors*, *Endocr. Rev.* 25 (2004) 235.
- [19] M. Manea, U. Leurs, E. Orbán, Z. Baranyai, P. Öhlschlager, A. Marquardt, Á. Schulcz, M. Tejada, B. Kapuvári, J. Tóvári, *Enhanced enzymatic stability and antitumor activity of daunorubicin-GnRH-III bioconjugates modified in position 4*, *Bioconjugate Chem.* 22 (2011) 1320.
- [20] G. Keller, A.V. Schally, T. Gaiser, A. Nagy, B. Baker, G. Westphal, G. Halmos, J.B. Engel, *Human malignant melanomas express receptors for luteinizing hormone releasing hormone allowing targeted therapy with cytotoxic luteinizing hormone releasing hormone analogue*, *Cancer Res.* 65 (2005) 5857.
- [21] C. Yates, S. Sharp, J. Jones, D. Topps, M. Coleman, R. Aneja, J. Jaynes, T. Turner, *LHRH-conjugated lytic peptides directly target prostate cancer cells*, *Biochem. Pharmacol.* 81 (2011) 104–110.
- [22] H. Guo, J. Lu, H. Hathaway, M.E. Royce, E.R. Prossnitz, Y. Miao, *Synthesis and*

- evaluation of novel gonadotropin-releasing hormone receptor-targeting peptides, *Bioconjug. Chem.* 22 (2011) 1682–1689.
- [23] J. Hu, S. Youssefian, J. Obayemi, K. Malatesta, N. Rahbar, W. Soboyejo, Investigation of adhesive interactions in the specific targeting of triptorelin-conjugated PEG-coated magnetite nanoparticles to breast cancer cells, *Acta Biomater.* (2018).
- [24] S.M. Alhamed, Design and anti-proliferative evaluation of triptorelin conjugated tris (4-methoxyphenyl) methanol derivatives, *Teaching Teacher Educ.* 18 (2015) 173–181.
- [25] S.N. Markovic, Targeted cancer therapy, *Nature* 432 (2004) 294–297.
- [26] F. Zhang, G. Zhu, O. Jacobson, Y. Liu, K. Chen, G. Yu, Q. Ni, J. Fan, Z. Yang, F. Xu, X. Fu, Z. Wang, Y. Ma, G. Niu, X. Zhao, X. Chen, Transformative nanomedicine of an amphiphilic camptothecin prodrug for long circulation and high tumor uptake in cancer therapy, *ACS Nano* 11 (2017) 8838–8848.
- [27] B. Sun, C. Luo, H. Yu, X. Zhang, Q. Chen, W. Yang, M. Wang, Q. Kan, H. Zhang, Y. Wang, Z. He, J. Sun, Disulfide bond-driven oxidation- and reduction-responsive prodrug nanoassemblies for cancer therapy, *Nano Lett.* 18 (2018) 3643–3650.
- [28] H. Jin, C. Wan, Z. Zou, G. Zhao, L. Zhang, Y. Geng, T. Chen, A. Huang, F. Jiang, J.P. Feng, Tumor ablation and therapeutic immunity induction by an injectable peptide hydrogel, *ACS Nano* 12 (2018).
- [29] C. Luo, J. Sun, D. Liu, B. Sun, M. Lei, S. Musetti, J. Li, X. Han, Y. Du, L. Li, Self-assembled redox dual-responsive prodrug-nanosystem formed by single thioether-bridged paclitaxel-fatty acid conjugate for cancer chemotherapy, *Nano Lett.* 16 (2016) 5401.
- [30] J. Wang, X. Sun, W. Mao, W. Sun, J. Tang, M. Sui, Y. Shen, Z. Gu, Tumor redox heterogeneity-responsive prodrug nanocapsules for cancer chemotherapy, *Adv. Mater.* 25 (2013) 3670–3676.
- [31] R.J. Aitken, L. Muscio, S. Whiting, H.S. Connaughton, B.A. Fraser, B. Nixon, N.D. Smith, G.N.D. Iulii, Analysis of the effects of polyphenols on human spermatozoa reveals unexpected impacts on mitochondrial membrane potential, oxidative stress and DNA integrity; implications for assisted reproductive technology, *Biochem. Pharmacol.* 121 (2016).
- [32] H. Zou, W.J. Henzel, X. Liu, A. Lutschg, X. Wang, Apaf-1, a human protein homologous to *C. elegans* CED-4, participates in cytochrome c-dependent activation of caspase-3, *Cell* 90 (1997) 405–413.
- [33] K. Kuida, T.F. Haydar, C.Y. Kuan, Y. Gu, C. Taya, H. Karasuyama, S.S. Su, P. Rakic, R.A. Flavell, Reduced apoptosis and cytochrome c-mediated caspase activation in mice lacking caspase 9, *Cell* 94 (1998) 325–337.
- [34] M.W. Lee, I. Hirai, H. Wang, Caspase-3-mediated cleavage of Rad9 during apoptosis, *Oncogene* 22 (2003) 6340–6346.
- [35] B. Yang, X. Li, C. Zhang, S. Yan, W. Wei, X. Wang, X. Deng, H. Qian, H. Lin, W. Huang, Design, synthesis and biological evaluation of novel peptide MC2 analogues from *Momordica charantia* as potential anti-diabetic agents, *Org. Biomol. Chem.* 13 (2015) 4551–4561.
- [36] C. Jian, P. Zhang, J. Ma, S. Jian, Q. Zhang, B. Liu, S. Liang, M. Liu, Y. Zeng, Z. Liu, The roles of fatty acid modification in the activity of anticancer peptide of R-lycosin-I, *Mol. Pharm.* (2018).